Fischer aminocarbene conformers containing a 2-thienyl or 2-furyl ring: a crystallographic, NMR, and DFT study

Marilé Landman, Roan Fraser, Linette Twigge & Jeanet Conradie

View supplementary material

Submit your article to this journal

View related articles

Citing articles: 1 View citing articles

Accepted author version posted online: 05 May 2015.
Published online: 30 Jun 2015.

Article views: 120

View Crossmark data

Taylor & Francis
Taylor & Francis Group

Fischer aminocarbene conformers containing a 2-thienyl or 2-furyl ring: a crystallographic, NMR, and DFT study

MARILÉ LANDMAN†*, ROAN FRASER†, LINETTE TWIGGE‡ and
JEANET CONRADIE‡*

†Department of Chemistry, University of Pretoria, Hatfield, South Africa
‡Department of Chemistry, University of the Free State, Bloemfontein, South Africa
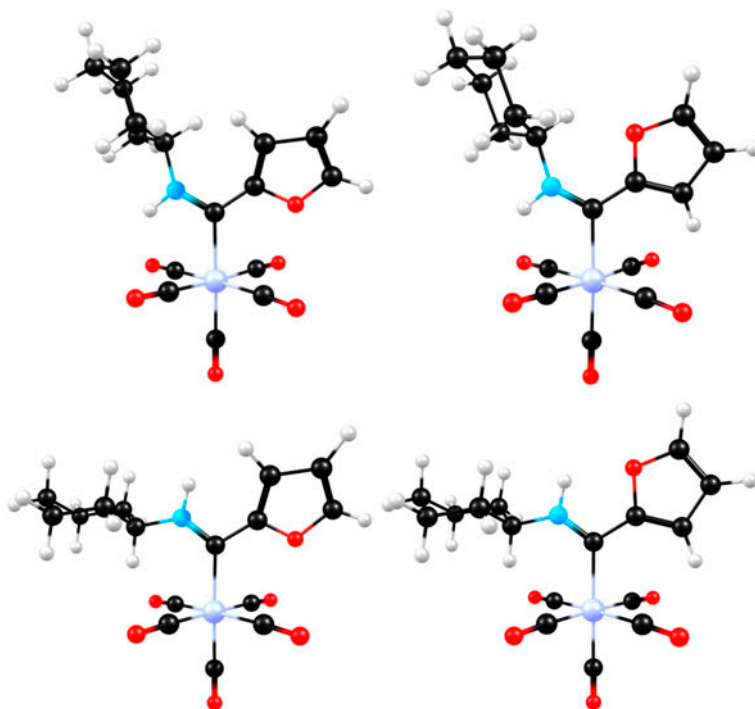
Fischer aminocarbene complexes $[(CO)_5M=C(NHR)Y]$ (M=Cr or W; R=H, Cy or $C_2H_4NH_2$; Y=2-thienyl or 2-furyl) containing an amino group exist as two isomers in solution, the **E** and **Z** isomers. The two isomers arise from restricted rotation about the N–$C_{carbene}$ bond, that exhibits double bond character due to π-donation from nitrogen to the carbene carbon. Each isomer exists as two conformers in fast equilibrium with each other. The conformers arise from the rotation of the aryl ring around the $C_{carbene}$–C_{aryl} single bond with a DFT calculated rotation barrier of 0.1–0.5 eV. The

---

*Corresponding authors. Email: marile.landman@up.ac.za (M. Landman); conradj@ufs.ac.za (J. Conradie)

main isomer, isolated in the solid state, generally exhibits a *syn* orientation of the aryl ring relative to the amino substituent and a *Z* configuration of the amino substituent relative to the metal.

Keywords: Fischer aminocarbene; Conformation; Isomer; DFT; NMR

1. Introduction

Electrophilic alkoxy Fischer carbene complexes are susceptible to nucleophilic attack on the carbene carbon [1–3]. Nucleophilic attack by amines (aminolysis) leads to substitution of the alkoxy substituent to form aminocarbene complexes [4, 5]. Aminocarbenes were synthesized not long after the first stable alkoxy carbene [6]. Aminocarbene complexes tend to be more stable than the corresponding alkoxycarbene and display fundamentally different behavior and reactivity [7]. Characteristically, the N–$C_{carbene}$ bond in aminocarbenes exhibits double bond character due to π-donation from nitrogen to the carbene carbon, see scheme 1. Due to restricted rotation about the N–$C_{carbene}$ bond, both *E* and *Z* configurations are observed for aminocarbene complexes [8–10]. Additionally, when the aminocarbene contains a heteroaryl ring such as 2-thienyl (Th) or 2-furyl (Fu), the orientation of the heteroatom (O or S) of the heteroaryl ring may be either facing away or toward the metal center (*syn* or *anti* to the amino substituent). This leads to four different conformers possible for heteroaryl ring-containing aminocarbene complexes, as illustrated in scheme 2.
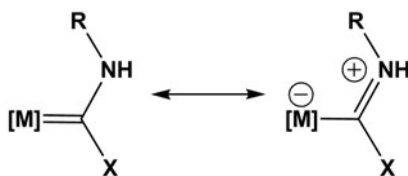
Scheme 1.   Resonance forms of the aminocarbene complexes; [M] = M(CO)$_5$ in this study
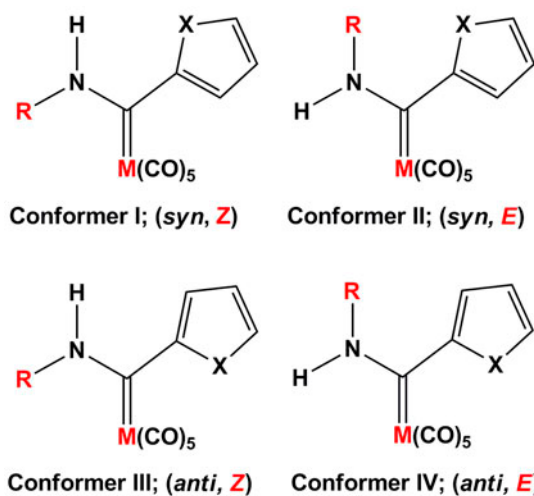
Scheme 2.   Conformers possible for aminocarbene complexes containing a heteroaryl ring such as 2-thienyl or 2-furyl. When R = H, only two conformers are possible: *syn* and *anti*.

Fischer assigned the stereochemistry of [(CO)$_5$M=C(NHMe)Y] (M=W or Cr; Y=Ph) and related complexes around the carbene carbon-nitrogen bond by employing ^{1}H NMR shifts of the α-hydrogens of the alkyl group on nitrogen that are downfield for the **Z**-isomers relative to those for the **E**-isomers [11, 12]. Crystal structures of the **E** and **Z** configurations of [(CO)$_5$W=C(NHMe)CHCHCH$_3$] confirmed the assignment of stereochemistry on the basis of the ^{1}H chemical shifts of the N-methyl (3.54 (**Z**) and 3.15 ppm (**E**)) [13]. Rudler *et al.* [14] observed a mixture of two isomers (**E** : **Z** 85 : 15) when reacting allylamine with [(CO)$_5$W=C(OEt)Me], which could be separated by refluxing the mixture in benzene. The **Z**-isomer formed a chelated complex and could be separated with column chromatography from the **E**-isomer. Crystal structure determinations confirmed the structures of both isomers. In all the cases mentioned, the R group of the complex was represented by an alkyl or aryl substituent. This situation becomes more complex if the R substituent is a heteroaryl ring.

The crystal structure of [(CO)$_5$W=C(NHCy)Th] showed disorder, consistent with conformers I and III (*syn* and *anti* orientation of the thienyl ring relative to the amino group) in scheme 2 [15]. This prompted the question of what the real structures of the two isomers observed in NMR spectra of Fischer aminocarbene conformers containing 2-thienyl or 2-furyl substituents are. In this regards we present here a combined crystallographic, NMR and density functional theory (DFT) study of Fischer aminocarbene complexes of the type [(CO)$_5$M=C(NHR)Y] (Y=2-thienyl or 2-furyl; R=cyclohexyl, H or ethylenediamine; M=Cr or W).

2. Experimental

2.1. *General*

All syntheses were carried out using standard Schlenk techniques under an inert atmosphere of nitrogen or argon. Solvents were dried prior to use. Triethyloxonium tetrafluoroborate was synthesized according to the literature method [16]. Nuclear magnetic resonance spectra were recorded on a Bruker AC-300 spectrometer or on a Bruker 600 MHz AVANCE II spectrometer in CDCl$_3$ or CD$_3$CN as solvent. ^{1}H NMR spectra were recorded at either 300.12 or 600.26 MHz and ^{13}C NMR spectra at either 75.47 or 150.94 MHz with the solvent signal as reference. 1D ^{1}H and proton decoupled ^{13}C NMR spectra, as well as 2D g-HSQC, g-HMBC, Phase-sensitive NOESY, DQF-COSY and 1D NOE experiments were recorded. Infrared spectra were recorded as KBr pellets on a Perkin Elmer Spectrum RX
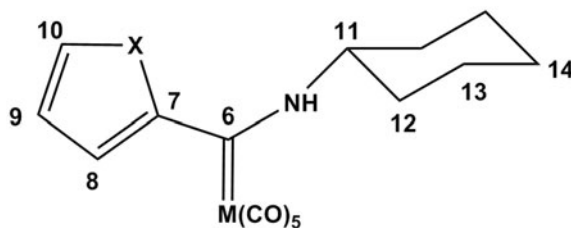
Scheme 3.   Atom numbering scheme for NMR spectra of **1**, **2**, **5** and **6**.
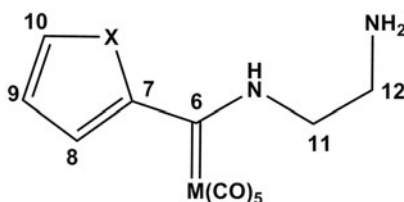
Scheme 4. Atom numbering scheme for NMR spectra of **3**, **4**, **7** and **8**.
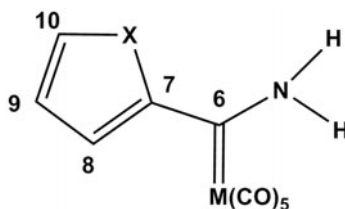
Scheme 5. Atom numbering scheme for NMR spectra of **9–12**.

FT-IR instrument and the vibrational bands of the carbonyl ligands in the region 1700–2200 cm^{-1} reported. Numbering schemes are shown in schemes 3–5.

2.2. *Synthesis*

The Cr-aminocarbene complexes [(CO)$_5$Cr=C(NHCy)Y] with Y=2-thienyl (**1**) or 2-furyl (**2**) [17] and [(CO)$_5$Cr=C(NHCH$_2$CH$_2$NH$_2$)Y] with Y=2-thienyl (**3**) or 2-furyl (**4**) were synthesized according to literature procedures [15]. [(CO)$_5$Cr=C(NHCH$_2$CH$_2$NH$_2$)Y] complexes with Y=2-thienyl (**3**) or 2-furyl (**4**) were synthesized according to a literature procedure for the analogous W(0) carbene complexes and are reported here for the first time [15].

Two isomers were observed on the NMR spectra for **1–8**.

2.2.1. [(CO)$_5$Cr=C(NHCy)Y] complexes with Y=2-thienyl (1) or 2-furyl (2). Complex (**A** in scheme 6) (0.332 g, 1.00 mmol) or (**B** in scheme 6) (0.316 g, 1.00 mmol) was dissolved in 20 mL of THF and cyclohexylamine (1.0 mmol, 0.100 g) was added in two portions over one hour. The solution was allowed to stir for 2 h, gradually changing color from dark red to bright yellow. Solvent was removed and a bright yellow crystalline solid was obtained. The product, **1** or **2**, was purified on a silica gel column with hexane:DCM gradient elution.

2.2.2. [(CO)$_5$Cr=C(NHCy)(2-thienyl)] (1): Isomer *A* (64.4%). ^{1}H NMR (600 MHz, CDCl$_3$): δ 8.41 (br s, NH), 7.38 (d, ^3J = 4.20 Hz, H10), 7.28 (d, ^3J = 1.67 Hz, H8), 7.03 (dd, ^3J = 4.20 Hz, ^3J = 1.67 Hz, H9), 4.50–4.35 (m, Hexyl-H11), 2.29–0.91 (Hexyl-ring). **Isomer *B* (35.6%):** ^{1}H NMR (600 MHz, CDCl$_3$): δ 8.78 (br s, NH), 7.35 (d, ^3J = 4.20 Hz, H10), 6.98 (dd, ^3J = 4.20 Hz, ^3J = 1.57 Hz, H9), 6.74 (d, ^3J = 1.57 Hz, H8), 3.74–3.61 (m, Hexyl-H11), 2.29–0.91 (Hexyl-ring). **Isomer *A*:** ^{13}C{^{1}H} NMR (151 MHz, CDCl$_3$): δ 256.24 (s, C6), 223.18 (s, COax), 217.43 (s, COeq), 155.78 (s, C7), 128.51 (s, C10),

128.21 (s, C9), 126.42 (s, C8), 62.70 (s, Hexyl-C11), 33.24 (s, Hexyl-C12), 24.94 (s, Hexyl-C14), 24.47 (s, Hexyl-C13). **Isomer B:** $^{13}C\{^1H\}$ NMR (151 MHz, CDCl$_3$): δ 270.03 (s, C6), 223.12 (s, COax), 217.16 (s, COeq), 148.59 (s, C7), 127.30 (s, C9), 126.31 (s, C10), 121.95 (s, C8), 69.91 (s, Hexyl-C11), 33.48 (s, Hexyl-C12), 24.74 (s, Hexyl-C14), 24.19 (s, Hexyl-C13). IR (KBr, cm^{-1}): ν_{CO} = 2054 (m), 1983 (vw), 1916 (s), 1872 (vs).

2.2.3. [(CO)$_5$Cr=C(NHCy)(2-furyl)] (2): Isomer A (55.7%). ^1H NMR (600 MHz, CDCl$_3$): δ 9.14 (br s, NH), 7.46 (br s, H10), 7.45 (br s, H8), 6.58 (br s, H9), 4.54–4.39 (m, Hexyl-H11), 2.24–1.15 (Hexyl-ring). **Isomer B (44.3%):** ^1H NMR (600 MHz, CDCl$_3$): δ 8.31 (br s, NH), 7.64 (s, H10), 7.13 (s, H8), 6.60 (s, H9), 4.19–4.05 (m, Hexyl-H11), 2.24–1.15 (Hexyl-ring). **Isomer A:** $^{13}C\{^1H\}$ NMR (151 MHz, CDCl$_3$): δ 238.81 (s, C6), 222.89 (s, COax), 218.04 (s, COeq), 157.16 (s, C7), 143.51 (s, C10), 124.94 (s, C8), 113.67 (s, C9), 62.08 (s, Hexyl-C11), 33.35 (s, Hexyl-C12), 24.56 (s, Hexyl-C13), 24.30 (s, Hexyl-C14). **Isomer B:** $^{13}C\{^1H\}$ NMR (151 MHz, CDCl$_3$): δ 247.93 (s, C6), 222.85 (s, COax), 217.94 (s, COeq), 155.94 (s, C7), 145.34 (s, C10), 122.74 (s, C8), 113.95 (s, C9), 61.15 (s, Hexyl-C11), 33.31 (s, Hexyl-C12), 25.01 (s, Hexyl-C13), 24.30 (s, Hexyl-C14). IR (KBr, cm^{-1}): ν_{CO} = 2054 (m), 1988 (vw), 1918 (s), 1884 (vs).

2.2.4. [(CO)$_5$Cr=C(NHCH$_2$CH$_2$NH$_2$)Y] complexes with Y=2-thienyl (3) or 2-furyl (4). Ethylenediamine (1.0 mmol, 0.061 g) was dissolved in 10 mL of DCM and complex (**A** in scheme 6) (0.332 g, 1.00 mmol) or (**B** in scheme 6) (0.316 g, 1.00 mmol) was added to the solution while maintaining vigorous stirring. The initial reaction mixture was dark red, but gradually became bright yellow. The solvent was removed, yielding a bright yellow crystalline solid, **3** or **4**, respectively.

2.2.5. [(CO)$_5$Cr=C(NHCH$_2$CH$_2$NH$_2$)(2-thienyl)] (3): Isomer A (86.9%). ^1H NMR (300 MHz, CD$_3$CN): δ 8.44 (br s, NH), 7.50 (dd, ^3J = 3.7 Hz, ^4J = 1.2 Hz, H10), 7.40 (dd, ^3J = 2.0, ^4J = 1.1 Hz, H8), 7.11 (dd, ^3J = 3.9, ^3J = 1.3 Hz, H9), 2.33–2.87 (m, H11, H12), 1.15 (br s, NH$_2$). **Isomer B (13.1%):** ^1H NMR (300 MHz, CD$_3$CN): δ 8.52 (br s, NH), 7.77 (dd, ^3J = 3.8 Hz, ^4J = 1.2 Hz, H10), 7.38 (dd, ^3J = 3.8, ^3J = 1.3 Hz, H9), 6.96 (dd, ^3J = 2.0, ^4J = 1.1 Hz, H8), 2.33–2.87 (m, H11, H12), 1.15 (br s, NH$_2$). $^{13}C\{^1H\}$ NMR (300 MHz, CDCl$_3$): δ 278.6 (s, C6), 221.2 (s, COax), 217.0 (s, COeq), 137.8 (s, C7), 129.9 (s, C10), 129.0 (s, C8), 127.8 (s, C9), 61.9 (s, C11), 41.0 (s, C12). IR (KBr, cm^{-1}): ν_{CO} = 2051 (m), 1995 (vw), 1918 (s), 1854 (vs).

2.2.6. [(CO)$_5$Cr=C(NHCH$_2$CH$_2$NH$_2$)(2-furyl)] (4): Isomer A (73.3%). ^1H NMR (300 MHz, CD$_3$CN): δ 10.09 (br s, NH), 7.59 (s, H10), 6.88 (s, H8), 6.55 (s, H9), 2.46–2.80 (m, H11, H12), 1.98 (br s, NH$_2$). **Isomer B (26.7%):** ^1H NMR (300 MHz, CD$_3$CN): δ 9.82 (br s, NH), 7.44 (s, H10), 6.38 (s, H8), 6.23 (s, H9), 2.46–2.80 (m, H11, H12), 1.98 (br s, NH$_2$). $^{13}C\{^1H\}$ NMR (75 MHz, CD$_3$CN): δ 220.3 (s, COax), 214.8 (s, COeq), 156.2 (s, C7), 144.0 (s, C10), 124.6 (s, C9), 135.4 (s, C8), 50.0 (s, C11), 43.2 (s, C12). IR (KBr, cm^{-1}): ν_{CO} = 2065 (m), 1980 (vw), 1924 (s), 1862 (vs).

The W-aminocarbene complexes [(CO)$_5$W=C(NHCy)Y] with Y=2-thienyl (**5**) or 2-furyl (**6**) and [(CO)$_5$W=C(NHCH$_2$CH$_2$NH$_2$)Y] with Y=2-thienyl (**7**) or 2-furyl (**8**) were synthesized as described previously [15].

2.2.7. [(CO)₅W=C(NHCy)(2-thienyl)] (5): Isomer *A* (87.7%). ¹H NMR (600 MHz, CDCl₃): δ 8.30 (br s, NH), 7.53 (dd, ^3J = 4.98 Hz, ^4J = 0.96 Hz, H10), 7.37 (dd, ^3J = 3.84 Hz, ^4J = 0.96 Hz, H8), 7.14 (dd, ^3J = 4.98 Hz, ^3J = 3.84 Hz, H9), 4.49–4.41 (m, Hexyl-H11), 2.20–1.37 (Hexyl-ring). **Isomer *B* (12.3%):** ¹H NMR (600 MHz, CDCl₃): δ 8.63 (br s, NH), 7.49 (dd, ^3J = 4.98 Hz, ^4J = 0.98 Hz, H10), 7.09 (dd, ^3J = 4.98 Hz, ^3J = 3.66 Hz, H9), 6.95 (dd, ^3J = 3.66 Hz, ^4J = 0.98 Hz, H8), 3.85–3.77 (m, Hexyl-H11), 2.20–1.37 (Hexyl-ring). **Isomer *A*:** ¹³C{¹H} NMR (151 MHz, CDCl₃): δ 235.18 (t, $^1J_{W\text{-}C}$ = 90.41 Hz, C6), 202.80 (t, $^1J_{W\text{-}C}$ = 127.10 Hz, COax), 198.25 (t, $^1J_{W\text{-}C}$ = 127.08 Hz, COeq), 157.05 (s, C7), 129.51 (s, C10), 127.86 (s, C9), 127.02 (s, C8), 64.88 (s, Hexyl-C11), 32.98 (s, Hexyl-C12), 24.91 (s, Hexyl-C14), 24.43 (s, Hexyl-C13). **Isomer *B*:** ¹³C{¹H} NMR (151 MHz, CDCl₃): δ 245.70 (t, $^1J_{W\text{-}C}$ = 90.41 Hz, C11), 203.46 (t, $^1J_{W\text{-}C}$ = 127.80 Hz, COax), 198.76 (t, $^1J_{W\text{-}C}$ = 127.80 Hz, COeq), 150.20 (s, C7), 127.85 (s, C10), 127.33 (s, C9), 124.27 (s, C8), 59.53 (s, Hexyl-C11), 33.36 (s, Hexyl-C12), 24.74 (s, Hexyl-C14), 24.21 (s, Hexyl-C13). IR (KBr, cm⁻¹): ν_CO = 2061 (m), 1972 (vw), 1950 (s), 1906 (vs).

2.2.8. [(CO)₅W=C(NHCy)(2-furyl)] (6): Isomer *A* (96.7%). ¹H NMR (600 MHz, CDCl₃): δ 8.88 (br s, NH), 7.63 (dd, ^3J = 1.77 Hz, ^4J = 0.43 Hz, H10), 7.33 (dd, ^3J = 3.63 Hz, ^4J = 0.43 Hz, H8), 6.52 (dd, ^3J = 3.63 Hz, ^3J = 1.77 Hz, H9), 4.38–4.27 (m, Hexyl-H11), 2.18–1.08 (Hexyl-ring). **Isomer *B* (3.3%):** ¹H NMR (600 MHz, CDCl₃): δ 8.07 (br s, NH), 7.63 (dd, ^3J = 1.77 Hz, ^4J = 0.53 Hz, H10), 7.33 (dd, ^3J = 3.63 Hz, ^4J = 0.53 Hz, H8), 6.55 (dd, ^3J = 3.63 Hz, ^3J = 1.77 Hz, H9), 4.14–4.05 (m, Hexyl-H11), 2.18–1.08 (Hexyl-ring). **Isomer *A*:** ¹³C{¹H} NMR (151 MHz, CDCl₃): δ 219.32 (t, $^1J_{W\text{-}C}$ = 90.41 Hz, C6), 202.38 (t, $^1J_{W\text{-}C}$ = 127.54 Hz, COax), 198.37 (t, $^1J_{W\text{-}C}$ = 126.70 Hz, COeq), 159.04 (s, C7), 144.05 (s, C10), 126.35 (s, C8), 113.77 (s, C9), 64.32 (s, Hexyl-C11), 33.15 (s, Hexyl-C12), 24.98 (s, Hexyl-C14), 24.49 (s, Hexyl-C13). **Isomer *B*:** ¹³C{¹H} NMR (151 MHz, CDCl₃): δ 225.61 (t, C6), 202.78 (t, $^1J_{W\text{-}C}$ = 122.20 Hz, COax), 199.15 (t, $^1J_{W\text{-}C}$ = 122.20 Hz, COeq), 157.62 (s, C7), 145.82 (s, C10), 126.57 (s, C8), 113.36 (s, C9), 61.11 (s, Hexyl-C11), 33.24 (s, Hexyl-C12), 24.98 (s, Hexyl-C14), 24.32 (s, Hexyl-C13). IR (KBr, cm⁻¹): ν_CO = 2059 (m), 1966 (vw), 1908 (s), 1882 (vs).

2.2.9. [(CO)₅W=C(NHCH₂CH₂NH₂)(2-thienyl)] (7) [15]: Isomer *A* (92.4%). ¹H NMR (600 MHz, CDCl₃): δ 9.45 (br s, NH), 7.48 (dd, ^3J = 5.03 Hz, ^4J = 1.09 Hz, H10), 7.38 (dd, ^3J = 3.80 Hz, ^4J = 1.09 Hz, H8), 7.08 (dd, ^3J = 5.03 Hz, ^3J = 3.80 Hz, H9), 3.89 (q, H11), 3.10 (q, H12), 1.70 (br, s, NH₂). **Isomer *B* (7.6%):** ¹H NMR (600 MHz, CDCl₃): δ 9.73 (br s, NH), 7.49 (dd, ^3J = 4.97 Hz; ^4J = 1.01 Hz, H10), 7.04 (dd, ^3J = 4.97 Hz, ^3J = 3.68 Hz, H9), 6.99 (dd, ^3J = 3.68 Hz, ^4J = 1.01 Hz, H8), 3.43 (q, H11), 2.94 (q, H12), 1.70 (br, s, NH₂). **Isomer *A*:** ¹³C{¹H} NMR (151MHz), CDCl₃: δ 237.41 (s, C6), 202.69 (s, COax), 198.55 (t, COeq, $^1J_{W\text{-}C}$ = 126.96 Hz), 156.94 (s, C7), 129.92 (s, C10), 128.12 (s, C9), 127.42 (s, C8), 55.99 (s, C11), 40.24 (s, C12). IR (KBr, cm⁻¹): ν_CO = 2059 (m), 1916 (vs).

2.2.10. [(CO)₅W=C(NHCH₂CH₂NH₂)(2-furyl)] (8) [15]: Isomer *A* (93.8%). ¹H NMR (600 MHz, CDCl₃): δ 9.84 (br s, NH), 7.59 (d, ^3J = 1.77 Hz, H10), 7.33 (d, ^3J = 3.65 Hz, H8), 6.51 (dd, ^3J = 3.65 Hz, ^3J = 1.77 Hz H9), 3.89 (q, H11), 3.07 (q, H12), 1.72 (br, s,

NH$_2$). **Isomer *B* (6.2%):** ^{1}H NMR (600 MHz, CDCl$_3$): δ 9.31 (br s, NH), 7.64 (d, ^3J = 1.46 Hz, H10), 7.21 (d, ^3J = 3.62 Hz, H8), 6.55 (dd, ^3J = 3.62 Hz, ^3J = 1.45 Hz, H9), 3.65 (q, H11), 3.01 (q, H12), 1.72 (br, s, NH$_2$). **Isomer *A*:** ^{13}C{^{1}H} NMR (151 MHz, CDCl$_3$): δ 222.98 (s, C6), 202.35 (s, COax), 198.62 (t, COeq, $^1J_{W\text{-}C}$ = 126.24 Hz), 159.57 (s, C7), 144.33 (s, C10), 125.78 (s, C8), 113.61 (s, C9), 55.86 (s, C11), 40.55 (s, C12). IR (KBr, cm^{-1}): ν$_{CO}$ = 2058 (m), 1972 (vw), 1910 (s), 1892 (vs).

The aminocarbene complexes [(CO)$_5$M=C(NH$_2$)Y] with M=Cr, Y=2-thienyl (**9**) or 2-furyl (**10**) and with M=W, Y = 2-thienyl (**11**) or 2-furyl (**12**) [18] were synthesized as described previously for **9** and **10** [19]. Only one isomer is observed on the NMR spectra.

2.2.11. [(CO)$_5$Cr=C(NH$_2$)(2-thienyl)] (9) [19]. ^{1}H NMR (300 MHz, CDCl$_3$): δ 8.20 (br s, NH$_2$), 7.62 (d, ^3J = 4.5 Hz, H10), 7.19 (dd, ^3J = 3.9 Hz, H9), 7.69 (d, ^3J = 3.9 Hz, H8). ^{13}C{^{1}H} NMR (75 MHz, CDCl$_3$): δ 268.3 (s, C6), 222.7 (s, COax), 217.4 (s, COeq), 151.4 (s, C7), 132.8 (s, C10), 129.0 (s, C9), 131.7 (s, C8). IR (KBr, cm^{-1}): ν$_{CO}$ = 2056 (m), 1977 (vw), 1947 (s), 1936 (vs).

2.2.12. [(CO)$_5$Cr=C(NH$_2$)(2-furyl)] (10) [19]. ^{1}H NMR (300 MHz, CDCl$_3$): δ 8.73 (br s, NH$_Z$), 8.16 (br s, NH$_E$), 7.55 (d, ^3J = 3.7 Hz, H10), 7.51 (br s, H8), 6.61 (dd, ^3J = 3.7 Hz, ^3J = 1.8 Hz, H9). ^{13}C{^{1}H} NMR (75 MHz, CDCl$_3$): δ 253.3 (s, C6), 223.3 (s, COax), 218.4 (s, COeq), 157.3 (s, C7), 145.5 (s, C10), 128.0 (s, C8), 114.5 (s, C9). IR (KBr, cm^{-1}): ν$_{CO}$ = 2060 (m), 1991 (vw), 1961 (s), 1946 (vs).

2.2.13. [(CO)$_5$W=C(NH$_2$)(2-thienyl)] (11). Yield: 88.6%: ^{1}H NMR (300 MHz, CDCl$_3$): δ 8.54 (br s, NH$_Z$), 8.07 (br s, NH$_E$), 7.71 (dd, ^3J = 5.1 Hz, ^4J = 1.2 Hz, H10), 7.66 (dd, ^3J = 3.9 Hz, ^4J = 1.2 Hz, H8), 7.22 (dd, ^3J = 5.0 Hz, ^3J = 3.9 Hz, H9). ^{13}C{^{1}H} NMR (75 MHz, CDCl$_3$): δ 244.3 (s, C6), 202.4 (s, COax), 198.4 (t, $^1J_{W\text{-}C}$ = 127.3 Hz, COeq), 153.5 (s, C7), 133.0 (s, C10), 132.8 (s, C8), 129.0 (s, C9). IR (KBr, cm^{-1}): ν$_{CO}$ = 2063 (m), 1921 (vw), 1889 (s), 1871 (vs).

2.2.14. [(CO)$_5$W=C(NH$_2$)(2-furyl)] (12): Yield: 79.3%. ^{1}H NMR (300 MHz, CDCl$_3$): δ 9.00 (br s, NH$_Z$), 7.96 (br s, NH$_E$), 7.60 (d, ^3J = 1.7 Hz, H8), 7.53 (d, ^3J = 3.6 Hz, 1H), 6.62 (dd, ^3J = 3.7 Hz, ^3J = 1.8 Hz, H9). ^{13}C{^{1}H} NMR (75 MHz, CDCl$_3$): δ 230.0 (t, $^1J_{W\text{-}C}$ = 88.0 Hz. C6), 202.5 (t, $^1J_{W\text{-}C}$ = 128.4 Hz, COax), 197.6 (t, $^1J_{W\text{-}C}$ = 127.2 Hz, COeq), 159.0 (s, C7), 145.6 (s, C10), 129.4 (s, C8), 114.5 (s, C9). IR (KBr, cm^{-1}): ν$_{CO}$ = 2009 (m), 1925 (m), 1889 (s), 1854 (vs).

2.3. Crystallography

Crystals suitable for single crystal X-ray crystallography were obtained for **1**, **2**, **7**, **11** and **12**. Single-crystal X-ray data were collected at 150 K on a Bruker D8 Venture kappa geometry diffractometer, with duo Iμs sources, a Photon 100 CMOS detector, and APEX II [20] control software using Quazar multilayer optics monochromated, Mo Kα radiation by means of a combination of φ and ω scans. Data reduction was performed using SAINT+ [20] and the intensities were corrected for absorption using SADABS [20]. The structures were solved by intrinsic phasing using SHELXTS [21] and refined by full-matrix least

squares using SHELXTL and SHELXL-2013 [21]. Ortep/POV-RAY drawings [22, 23] of the five structures are included in figures 1–5 with ADP's at the 50% probability level. All non-hydrogen atoms were refined with anisotropic displacement parameters. All isotropic displacement parameters for hydrogens were calculated as $X \times U$eq of the atom to which they are attached; $X = 1.5$ for the methyl hydrogens and 1.2 for all other hydrogens. Data collection, structure solution, and refinement details are available in each CIF file. The crystal structures have been deposited at the Cambridge Crystallographic Data Center and allocated the deposition numbers: CCDC 1051512–1051516 for **1**, **2**, **7**, **11** and **12**, respectively.

2.4. *DFT*

DFT calculations were performed both with the hybrid functional B3LYP [24, 25] as implemented in the Gaussian 09 program package [26] and with the PW91 [27] Generalized Gradient Approximation functional as implemented in the Amsterdam Density Functional 2013 program [28–30] using a TZP (Triple ζ polarized) basis set (in Gaussian 6-311G(d, p) on all atoms and def2svp [31] for the metal (W or Cr)). Geometries of complexes were optimized in the gas phase with no constraint unless explicitly specified.

3. Results and discussion

3.1. *Synthesis of the complexes*

Classic Fischer methodology was employed in the synthesis of the carbene starting materials (**A-D**) (scheme 6) [32–34]. Deprotonation of the heteroaromatic ring with *n*-BuLi
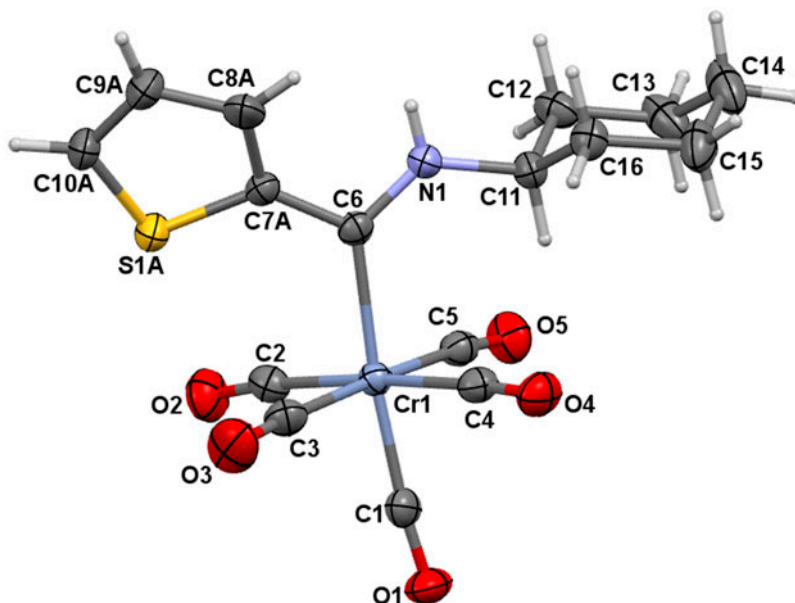

Figure 1. A perspective drawing of the molecular structure of 1 showing the atom numbering scheme. ADPs are shown at the 50% probability level.
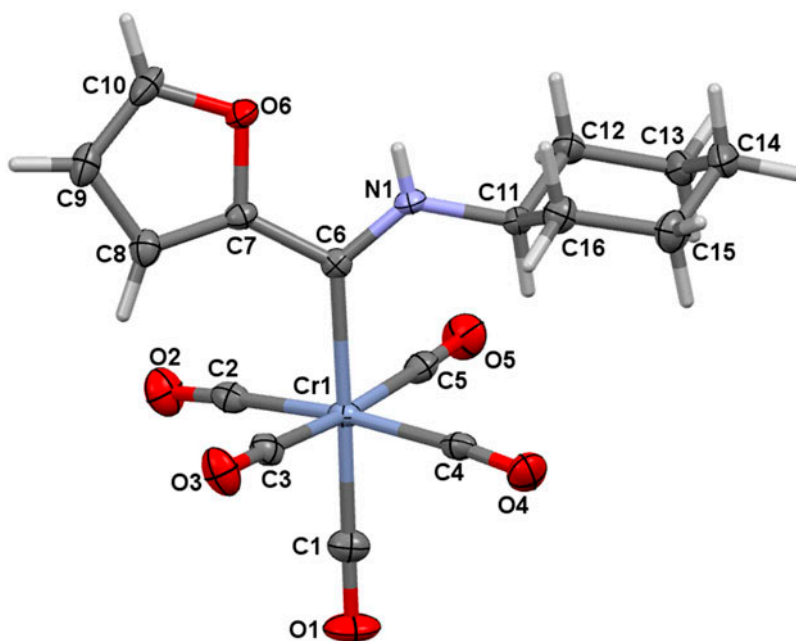
Figure 2. A perspective drawing of the molecular structure of **2** showing the atom numbering scheme. ADPs are shown at the 50% probability level.

at −78 °C in THF, followed by addition of one equivalent of $M(CO)_6$ and the subsequent alkylation with EtO_3BF_4 yielded the orange monocarbene complexes (**A–D**) after purification by column chromatography. Complexes **1–8** were synthesized by stirring the starting material (**A–D**) and the relevant amine (cyclohexylamine or ethylenediamine) to substitute the ethoxy substituent with an amino substituent (scheme 6) [15]. Aminolysis of **9–12** was achieved by bubbling ammonia gas through a solution of the appropriate ethoxy carbene complex dissolved in ether. A color change from orange to yellow for the reaction mixture indicated completion of the reaction. The yields of these reactions are high as aminolysis typically proceeds almost quantitatively.

3.2. NMR characterization of the complexes

For **1–8**, two isomers were observed in the NMR spectra, denoted isomer **A** for the major isomer and isomer **B** for the minor isomer in each case. However, for the W-aminocarbene complexes the ratio difference between the two isomers was much more prominent than for the Cr-aminocarbene complexes.

A COSY NMR spectrum was used to assign resonances to the H10, H9 and H8 positions (see experimental section for the atom numbering) of the thienyl and furyl rings of both the chromium and tungsten complexes. For the furyl rings of both metals, H8 was shifted more downfield than H9 for both isomers, while for the thienyl rings, H8 was shifted more downfield than H9 for isomer **A**, but for isomer **B** H9 was shifted more downfield than H8. In addition, for the thienyl ring complexes the amino proton is shifted more upfield for isomer
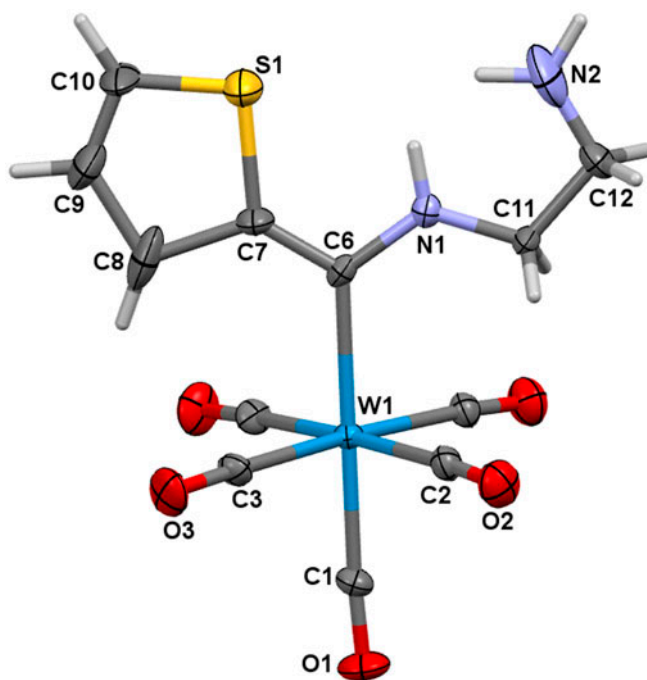
Figure 3. A perspective drawing of the molecular structure of **7** showing the atom numbering scheme. ADPs are shown at the 50% probability level.
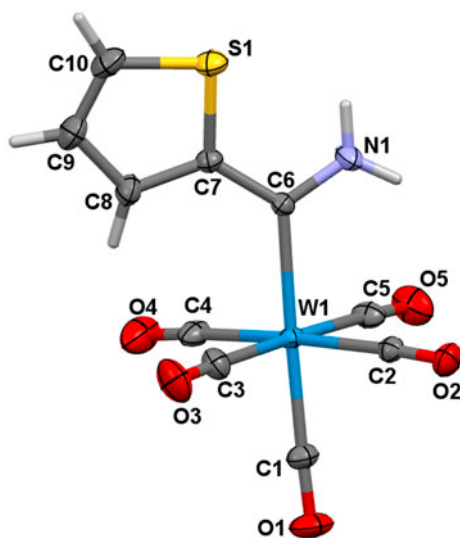
Figure 4. A perspective drawing of the molecular structure of **11** showing the atom numbering scheme. ADPs are shown at the 50% probability level.
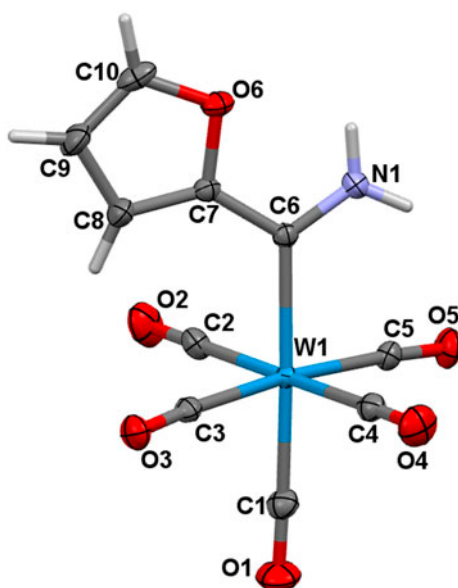
Figure 5. A perspective drawing of the molecular structure of **12** showing the atom numbering scheme. ADPs are shown at the 50% probability level.
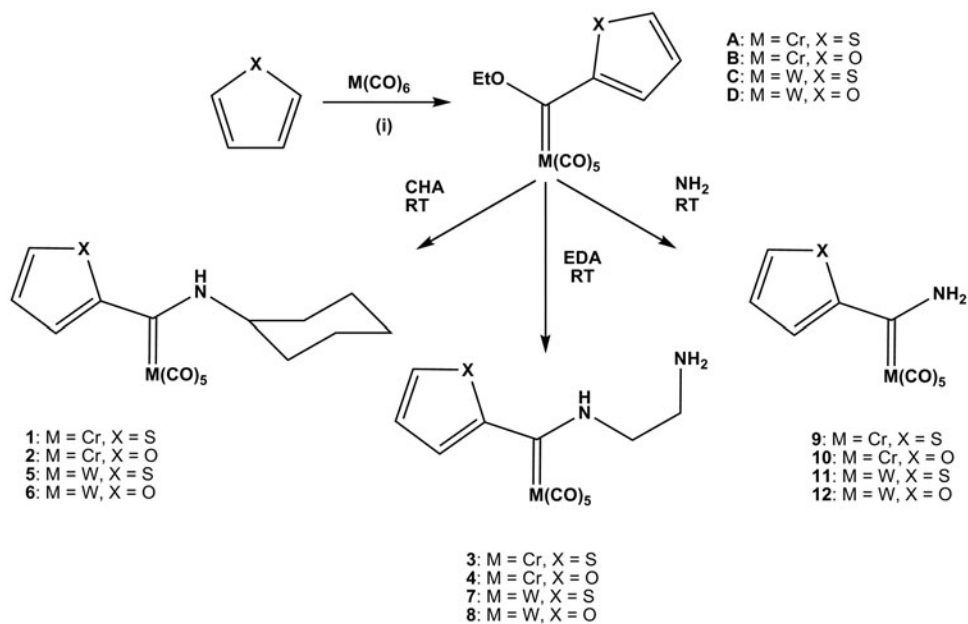
Scheme 6. Synthetic route for the synthesis of aminocarbene complexes. Reagents and conditions: (i) For M = Cr: a. 1.1 eq. n-BuLi, THF, −20 °C; b. 1 eq. Cr(CO)$_6$, thf, −40 °C; c. Et$_3$OBF$_4$, CH$_2$Cl$_2$, −20 °C; For M = W: a. 1.1 eq. *n*-BuLi, THF, −20 °C; b. 1 eq. W(CO)$_6$, thf, −40 °C; c. Et$_3$OBF$_4$, CH$_2$Cl$_2$, −20 °C.

A than for isomer *B*, while the opposite was observed for the furyl ring complexes. These differences in chemical shifts for H8, H9 and amino protons between the different isomers of the furyl and thienyl ring complexes suggest that sulfur has a bigger influence than oxygen on the chemical environment experienced by the H8, H9 and amino protons in the conformation adapted by isomer *B*.

The ^3J coupling constants between H10 and H9 are also much bigger for the thienyl rings than for the furyl rings (~4–5 Hz compared to 1–2 Hz) which correlate with the lower electronegativity of sulfur (2.58), compared to oxygen (3.44) [35], as well as the atom distances between these two protons that are smaller for the thienyl rings than for the furyl rings.

Assignment of the ^{13}C NMR resonances was done using HSQC and HMBC spectra. From the chemical shifts of the carbene carbons, it can be seen that for the chromium complexes, the carbene carbon is less shielded than for the tungsten complexes and hence resonates at a lower field. This same trend of shielding was observed for the CO resonances.

When the carbene carbon chemical shifts of the furyl and thienyl ring complexes are compared, the carbene carbons lay more upfield for the furyl ring ligands. Also, the C10 carbons of the furyl rings are much more downfield than that of the thienyl rings, while C9 carbons are much more upfield for the furyl rings when compared to the thienyl; this pattern was also observed for 2-furyl- and 2-thienylcarbenium ion derivatives [36].

It was previously mentioned that Fischer assigned the stereochemistry about carbene carbon-nitrogen bonds by ^1H NMR shifts of the α-hydrogens of the alkyl group on the nitrogen that are downfield for the *Z*-isomers relative to those for the *E*-isomers [2]. Comparison of the various chemical shifts of the Hexyl-H11 resonances of the compounds in this study indicate that isomers *A* have a *Z*-configuration about the carbene carbon-nitrogen bond, while isomers *B* have an *E*-configuration about the carbene carbon–nitrogen bond. These assignments were further proven by the 1D nuclear overhauser enhancement (NOE) spectra of $[(CO)_5Cr=C(NHCy)(2\text{-thienyl})]$ (**1**) and $[(CO)_5Cr=C(NHCy)(2\text{-furyl})]$ (**2**). The observed NOE correlations between H8 and NH hydrogen of isomer *A* can only be possible for a *Z*-configuration (conformer III in scheme 2), while NOE correlations between H8 and Hexyl-H11 of isomer *B* indicated an *E*-configuration (conformer IV in scheme 2), see figure 6.

No dynamic equilibrium exists between isomer *A* and isomer *B*, since ^1H NMR spectra recorded at different temperatures (a range from −60 to 50 °C), as well as different concentrations, did not show any change in the ratio between the isomers. Samples from the same batch of synthesis always showed the same *A* : *B* ratio. However, samples of the same complex, but from different synthesis batches, exhibit different *A* : *B* ratios in solution. This indicates that once the complex is synthesized, the ratio *A* : *B* is fixed and cannot be changed. The ratio *A* : *B* thus seems to be a consequence of the crystallization process.

The ratio of interproton distances in rigid molecules can be determined by the ratio of the intensities of a pair of NOE signals η_1/η_2 within the 1D NOE spectrum of the complex by the equation

$$\eta_1/\eta_2 = r_2^6/r_1^6$$

where η_1 = integral of proton 1, η_2 = integral of proton 2, r_1 = distance between proton 1 and irradiated peak for which the integral was arbitrarily assigned a value of 1000 and r_2 = distance between proton 2 and irradiated peak. If one of the distances r_1 or r_2 is known, the other distance can thus be determined [37]. We used the NOE integral ratio
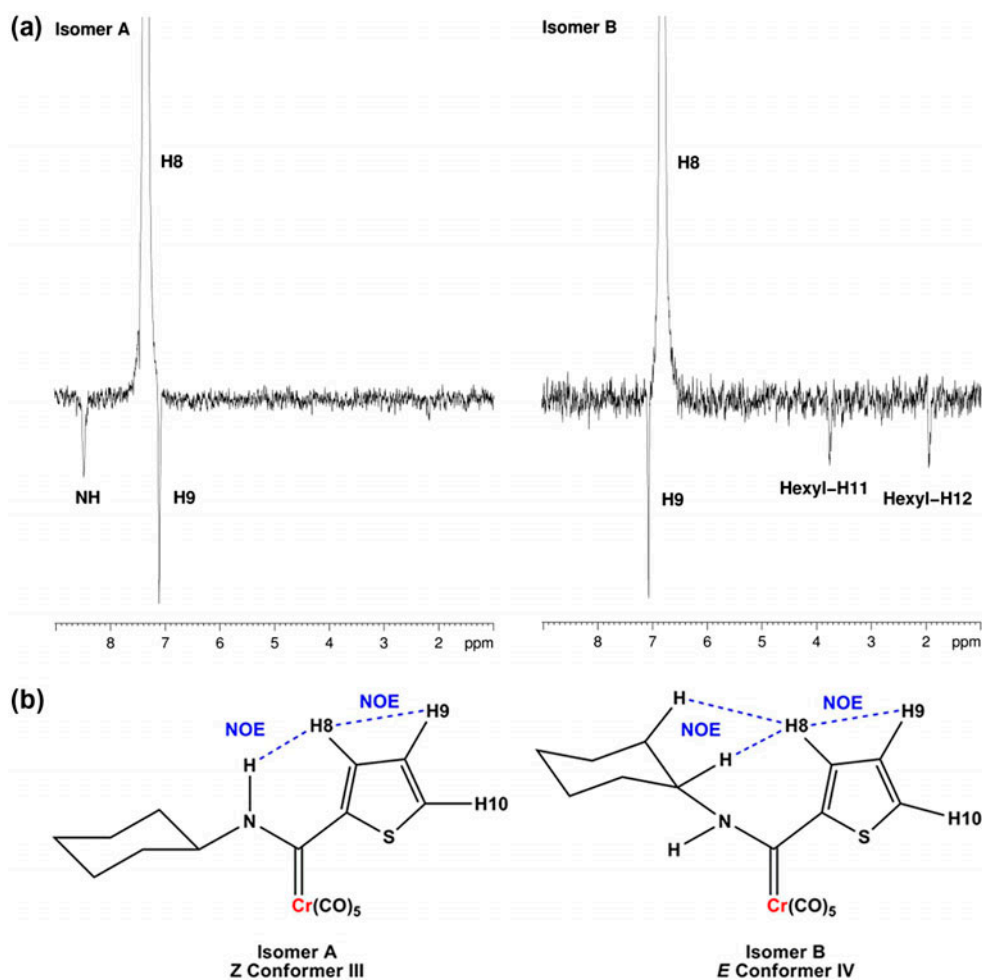
Figure 6. (a) 1D NOE spectra for **1** showing selected NOE correlations, highlighted in the structures (b).

Table 1. Interatomic distances obtained from NOE integrals and DFT optimized geometries of isomers *A* and *B* of **1**, [(CO)$_5$Cr=C(NHCy)(2-thienyl)].

Isomer	Conformer	r$_1$ (H9–H8) obtained from DFT	r$_2$ (H8–H$_{NH}$) obtained from DFT	r$_2$ (H8–H$_{NH}$) calculated from 1D NOE integrals
1*A*	III	2.622	2.211	2.650
			r$_2$ (H8–Hexyl-H11) obtained from DFT	**r$_2$ (H8–Hexyl-H11) calculated from 1D 1NOE integrals**
1*B*	IV	2.621	2.414	2.740

(η_1/η_2) of H$_{NH}$ and H9 and the DFT calculated H8–H9 distance for isomer *A*, conformer III of **1** to calculate the H$_{NH}$–H8 distance in III. The results are given in table 1. We observe that the H$_{NH}$–H8 distance obtained from the NOE integral ratio differs largely from the DFT calculated values. This result is consistent with the fact that isomer *A* of **1** is not a

rigid molecule in solution, but that the thienyl ring in conformer III of **1** rotates in solution, interchanging with conformer I (scheme 2). In this case, isomer *A* of **1** exhibits multiple conformations in solution that are interconverting rapidly on the NMR time-scale. This conformational exchange leads to an ensemble-averaging of the observed NOEs for each corresponding interproton distance in each contributing conformer. This result is thus consistent with isomer *A* observed in the NMR to be conformer I (*syn,Z*) and III (*anti,Z*) interconverting rapidly with each other. The DFT calculated barrier for the rotation of the thienyl ring from conformer I to conformer III in **1** is 0.16 eV (see DFT section below), low enough to allow for the rotation. This result is also consistent with the fact that the solid state crystal (see crystal structure section below) of **1** crystallized with a disorder of the thienyl ring as 55% *anti,Z* and 45% *syn,Z*.

The NOE integral ratio (η_1/η_2) of H9 and Hexyl-H11 and the DFT calculated H8–H9 distance for isomer *B*, conformer IV of **1** is used to calculate the H8–Hexyl-H11 distance in IV (results are in table 1). A similar result as discussed above is obtained, consistent with isomer *B* observed on the NMR to be conformer II and IV interconverting rapidly with each other.

The interpretation that isomer *A* observed on the NMR spectra is conformer I and III and isomer *B* observed on the NMR spectra is conformer II and IV interconverting rapidly from one to the other is also consistent with the fact that for **9–12** containing a symmetrical amino substituent (NH$_2$), only one isomer is observed in the NMR spectra. The *syn* and *anti* orientations of the aryl ring in **9–12** are also interconverting rapidly, since the DFT calculated rotation barrier of the aryl ring was calculated as 0.2–0.5 eV (see DFT section below).

3.3. *Crystal structures*

Suitable crystals of **1**, **2**, **7**, **11** and **12** were obtained from dichloromethane:hexane (1 : 1) solutions and molecular structures determined with single-crystal X-ray diffraction analysis. These structures of **1**, **2**, **7**, **11** and **12** were compared to the known structures of **5** [15], **6** [15], **8** [15], **9** [19] and **10** [19]. The atom labeling of the structures is shown in figures 1–5. Selected bond lengths, angles and torsion angles of the structures can be found in table 2.

Heterocyclic carbene complexes are usually characterized by planarity of the heteroaryl ring, metal, carbene carbon and the heteroatom (O or N) of the carbene substituent [15, 38, 39]. In this study, this holds in most cases, especially for the complexes containing a 2-furyl ring, which only deviates by 7° from planarity (in **2**), at most. By comparison, the 2-thienyl ring tends to be twisted out of this plane for most of the complexes with a thienyl substituent, with a maximum value of 37° for **1**. Only **7** shows planarity, with an M–C6–C7–S1 dihedral angle of 180°. The crystal structure of **7** yielded only one acceptable solution, which is in the orthorhombic space group Ama2. The consequence of this solution is that the N1–C11–C12–N2 side chain is exactly planar as this group, and the thienyl ring, lie in the crystallographic *bc*-mirror plane, perpendicular to the *a*-axis.

The crystal structure of **1** has some disorder in the orientation of the thienyl ring. The ring adopts two possible orientations and the relative occupancy of the positions of C7, C8, C9, C10 and S1 in the two orientations was refined to a ratio of 0.549 : 0.451. The major component is shown in figure 1.

The O6…HN1 distances in **2**, **6**, **10** and **12**, all 2-furyl complexes, are in general ~0.3 Å shorter (2.158–2.187 Å) than the corresponding S1…HN1 distance in the 2-thienyl complexes (2.408–2.487 Å). This additional stabilization due to hydrogen

Table 2. Selected geometric and crystallographic data of **1**, **2** and **5–12**.

	1	2	5	6	7	8	9	10[d]	11[a,d]	12[a,d]
Bond length (Å)										
M1–C6	2.128(4)	2.120(1)	2.269(5)	2.251(4)	2.266(4)	2.240(1)	2.096(1)	2.092(1) / 2.089(1)	2.240(3)	2.222(2)
M1–CO1	1.848(5)	1.862(2)	2.006(5)	2.000(4)	2.011(4)	2.010(2)	1.874(1)	1.876(2) / 1.878(1)	1.994(4)	2.021(2)
M1–COcis[a]	1.900(5)	1.901(2)	2.048(4)	2.040(4)	2.043(9)	2.037(2)	1.902(20)	1.896(2) / 1.899(2)	2.040(4)	2.041(2)
C6–C7	1.476(6)[a]	1.465(2)	1.473(6)	1.466(5)	1.340(16)	1.453(3)	1.466(2)	1.452(2) / 1.450(2)	1.455(5)	1.452(3)
C7–C8	1.389(6)[a]	1.359(2)[a]	1.411(12)	1.350(5)	1.570(19)	1.373(3)	1.420(2)	1.359(2) / 1.348(2)	1.495(5)	1.361(3)
C8–C9	1.392(6)[a]	1.423(2)[a]	1.451(12)	1.424(5)	1.482(16)	1.428(3)	1.420(2)	1.419(2) / 1.422(2)	1.436(6)	1.424(4)
C9–C10	1.390(6)[a]	1.341(2)	1.335(8)	1.336(6)	1.279(18)	1.337(4)	1.359(2)	1.333(2) / 1.322(3)	1.36(1)	1.340(5)
C10–S1/O6	1.724(6)[a]	1.361(2)	1.590(7)	1.362(4)	1.649(15)	1.369(3)	1.691(2)	1.358(2) / 1.364(2)	1.662(6)	1.358(3)
C7–S1/O6	1.745(6)[a]	1.387(9)	1.701(6)	1.392(4)	1.840(9)	1.381(3)	1.736(1)	1.387(1) / 1.388(2)	1.717(4)	1.382(3)
C6–N1	1.314(5)	1.312(2)	1.330(5)	1.320(5)	1.419(16)	1.313(3)	1.318(2)	1.315(2) / 1.316(2)	1.317(5)	1.314(3)
Bond angle (°)										
C1–M1–C6	175.0(2)	178.6(6)	177.43(18)	177.81(14)	179.8(7)	178.82(8)	175.5(1)	177.9(1) / 176.1(1)	177.48(14)	176.43(10)
M1–C6–N1	126.3(3)	127.7(2)	125.5(3)	127.3(3)	125.0(8)	126.29(14)	121.1(1)	123.4(1) / 122.0(1)	120.7(3)	123.09(17)
M1–C6–C7	122.9(5)[a]	121.0(1)	122.3(3)	120.8(3)	121.9(9)	122.51(13)	125.6(1)	124.2(1) / 125.4(1)	125.4(2)	124.36(16)
N1–C6–C7	110.6(5)[a]	111.2(1)	112.2(4)	111.9(3)	113.1(4)	111.19(17)	113.1(2)	112.4(1) / 112.6(1)	114.(3)	112.53(19)
Torsion angle (°)										
N1–C6–C7–S1/O6	148.8(6)[b,c] / −30.1(12)[b]	6.1(2)	0.000(2) / 180.000(1)[b]	6.1(4)	0.000(2)	0.2(3)	−21.3(2)	6.0(2) / −2.0(2)	−15.0(5)	−5.9(3)
M1–C6–N1–C11	1.3(6)	−5.5(2)	0.000(1)	−4.9(5)	0.000(2)	4.7(3)	–	–	–	–

(*Continued*)

Table 2. (*Continued*).

	1	2	5	6	7	8	9	10[d]	11[a,d]	12[a,d]
M1–C6–C7–S1/O6	−37.3(11)[b,c]	−173.4(1)	180.000(1) 0.000(2)	−172.2(2)	180.000 (1)	178.97 (14)	153.73 (7)	−173.58 (9) 177.1(1)	165.31 (19) 161.4(2)	174.33(14) −176.16 (17)
	146.8(6)[b]									
Conformation	55% *anti,Z*; 45% *syn, Z*	*syn,Z*	56% *syn,Z*; 44% *anti, Z*	*syn,Z*	*syn,Z*	*syn,Z*	*syn*	*syn*	*syn*	*syn*
Ref.	This study	This study	[15]	[15]	This study	[15]	[19]	[19]	This study	This study

[a]Average values.
[b]Two values due to disordered thienyl ring.
[c]Value for the major component.
[d]Two molecules in the asymmetric unit.

bonding, together with the planarity argument and the difference in electronegativity (O > S), may explain the higher rotational barrier determined for the 2-furyl complexes in the DFT study (see table 3).

Table 3. Selected results for conformations I–IV of **1–12**.

| Complex | Conformation | DFT calculated relative energy (eV) | | % NMR | X-ray structure | DFT calculated rotation barrier of aryl ring (eV) |
		PW91	B3LYP			PW91
1	I: *syn,Z*	**0.00**	**0.00**	64.4	45% disorder	0.16
	III: *anti Z*	0.04	0.04		55% disorder	
	II: *syn,E*	0.06	0.06	35.6		0.15
	IV: *anti,E*	0.08	0.08			
2	*syn,Z*	**0.00**	**0.00**	55.7	Crystal structure	0.37
	anti,Z	0.13	0.12			
	syn,E	0.13	0.12	44.3		0.20
	anti,E	0.17	0.18			
3	*syn,Z*	**0.00**	**0.00**	86.9	–	0.18
	anti,Z	0.05	0.05			
	syn,E	0.06	0.13	13.1		0.15
	anti,E	0.08	0.07			
4	*syn,Z*	**0.00**	**0.00**	73.3	–	0.37
	anti,Z	0.10	0.09			
	syn,E	0.09	0.08	26.7		0.26
	anti,E	0.13	0.12			
5	*syn,Z*	**0.00**	**0.00**	87.7	56% disorder	0.18
	anti,Z	0.03	0.03		44% disorder	
	syn,E	0.11	0.10	12.3		0.09
	anti,E	0.12	0.11			
6	*syn,Z*	**0.00**	**0.00**	96.7	Crystal structure	0.38
	anti,Z	0.13	0.14			
	syn,E	0.16	0.15	3.3		0.25
	anti,E	0.21	0.22			
7	*syn,Z*	**0.00**	**0.00**	92.4	Crystal structure	0.17
	anti,Z	0.03	0.04			
	syn,E	0.09	0.08	7.6		0.14
	anti,E	0.10	0.08			
8	*syn,Z*	**0.00**	**0.00**	93.8	Crystal structure	0.38
	anti,Z	0.11	0.10			
	syn,E	0.12	0.10	6.2		0.29
	anti,E	0.17	0.16			
9	*syn*	**0.00**	**0.00**	–	Crystal structure	0.23
	anti	0.05	0.06			
10	*syn*	**0.00**	**0.00**	–	Crystal structure	0.48
	anti	0.14	0.14			
11	*syn*	**0.00**	**0.00**	–	Crystal structure	0.28
	anti	0.04	0.05			
12	*syn*	**0.00**	**0.00**	–	Crystal structure	0.51
	anti	0.14	0.15			

The asymmetric units of **11** and **12** each have two molecules. In **11** intermolecular hydrogen bonding between oxygens of carbonyl groups of one molecule and the N–H of the other molecule is observed (2.186–2.373 Å). Similar bonding in **12** ranges from 2.343 to 2.402 Å for NH…OC interactions.

Due to the steric effect of the *Z* configuration in **1**, **2** and **5–8**, the M–C6–N1 angle is noticeably larger (125.0–127.7°) than the other two angles around C6. For **9–12**, this angle is smaller (120.7–123.4°) while the M1–C6–C7 angle is now the largest (124.2–125.6°).

3.4. *DFT study*

DFT calculations were used to optimize the four possible conformers (figure 7, scheme 2) of **1-12**, see table 3 for selected DFT data. The lowest energy conformer in each case was conformer I (*syn,Z*), the same conformer as was characterized by X-ray crystallography for
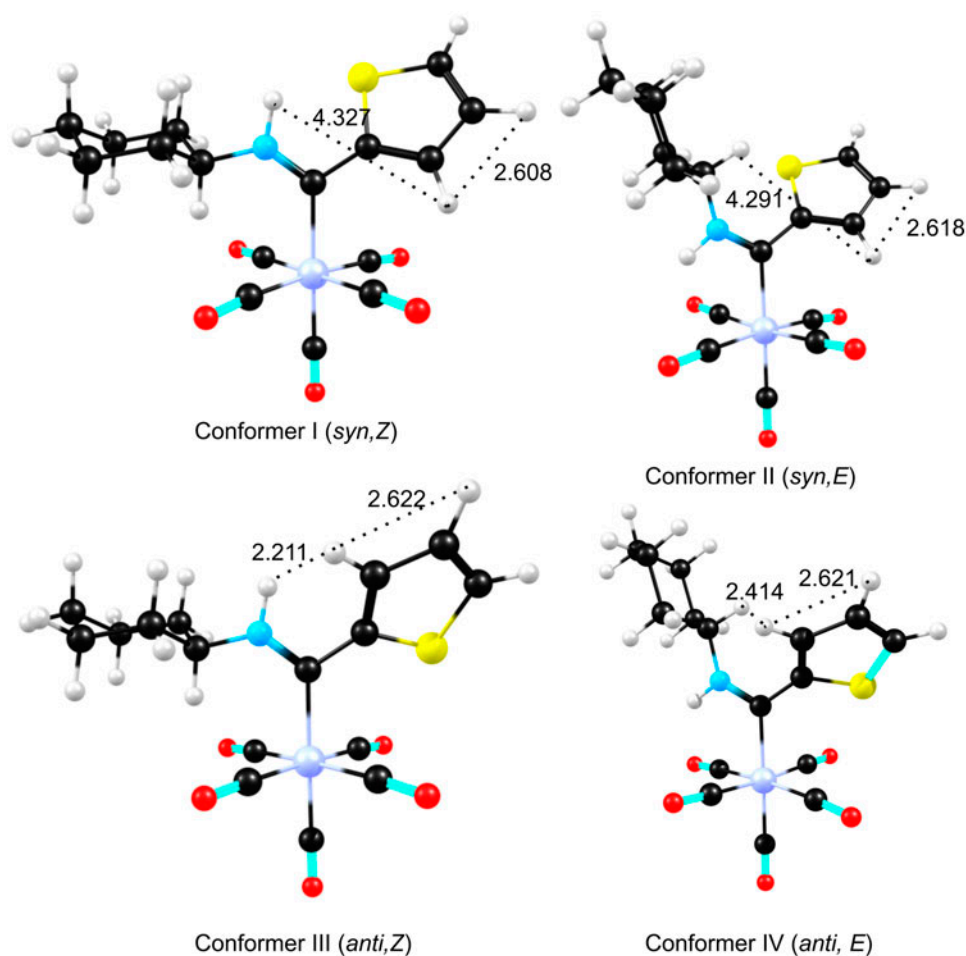

Figure 7. DFT optimized geometries of conformers I–IV of **1** showing selected interproton distances. Color code (online version): Cr (purple), C (black), S (yellow), N (cyan), O (red) and H (white) (see http://dx.doi.org/10.1080/00958972.2015.1046852 for color version).

1, **2** and **5–8**. The conformer with the second lowest DFT calculated energy is conformer III (*anti*,Z) which we propose to be in a fast dynamic equilibrium with conformer I, unfortunately too fast to distinguish from conformer I on the NMR time scale, even at −60 °C. The disorder found in the orientation of the thienyl ring of the X-ray structures of **1** and **5** is in agreement with this proposal. DFT results are thus consistent with isomer *A* existing as a fast equilibrium of the Z conformers I and III.

Figure 8 displays the change in energy of isomer *A* of **3** and **4** as a function the Cr–C6–C7–C8 dihedral angle in changing the aryl ring from the *syn* to the *anti*-orientation. The barrier of rotation for **1–12** is included in table 3. In agreement with the X-ray structures of aminocarbenes containing an aryl ring, the two lowest energy orientations of the furyl ring in these complexes are for Cr–C6–C7–C8=0° or 180°, while for the thienyl ring Cr–C6–C7–C8 it is *ca.* 30° and 140°, see figure 8 as representative example. From table 3 we observe that the barrier of rotation of the aryl ring is not influenced by the metal (Cr or W). The barrier of rotation of a furyl ring (0.2–0.5 eV) is on average 0.2 eV larger than that of the thienyl ring (0.1–0.3 eV) for related complexes. The rotation barrier of the *Z* isomers is generally higher than that of the *E* isomers.

The DFT calculated relative energies of conformers II and IV are within 0.22 eV of that of conformers I and III, implying that these conformers can also exist in observable quantities. From the NMR study, the geometry of isomer *B* is consistent with that of conformer IV. Since the rotation barrier of the aryl ring in conformers II and IV is low (<0.3 eV, table 3), DFT results are consistent with isomer *B* existing as a fast equilibrium of the *E* conformers II and IV.

Since there is no dynamic equilibrium found between isomers *A* and *B* in the temperature range −60 to +55 °C, and since different batches of **1–8** exhibit different ratios of isomers *A* and *B*, we propose that the ratio found between the two isomers is a consequence of crystallization conditions.
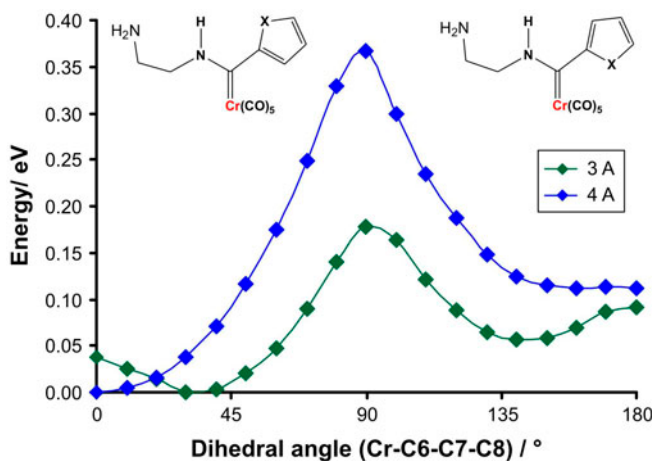

Figure 8. Potential energy curve of isomer *A* (Z orientation) of **3** and **4** as a function of the aryl ring rotation (Cr–C6–C7–C8 dihedral angle), 0° corresponds to the *syn,Z* and 180° corresponds to the *anti,Z* conformation.

4. Conclusion

Combined NMR, solid state X-ray crystallography and DFT study show that for Fischer aminocarbene (NHR with R ≠ H) complexes, both the *Z* and the *E* conformers of the amino group relative to the carbene-carbon exist in solution and can be distinguished in the NMR. The *syn* and *anti* orientations of the aryl ring relative to the heteroatom in Fischer aminocarbene conformers containing a 2-thienyl or 2-furyl ring interconverts rapidly with each other and cannot be distinguished on the NMR scale.

Supplementary material

CCDC 1051512-1051516 contain the supplementary crystallographic data for this article. Copies of the information may be obtained free of charge from the Director, CCDC, 12 Union Road, Cambridge CB2 1EZ, UK (Fax: +44 1223 336033; Email: deposit@ccdc. cam.ac.uk or www.ccdc.cam.ac.uk). The optimized coordinates of the DFT calculations of conformations I-IV of **1–8** and the *syn* and *anti* conformations of **9–12** are provided in the electronic supplementary information.

Disclosure statement

The authors declare no conflict of interest.

Supplemental data

Supplemental data for this article can be accessed here [http://dx.doi.org/10.1080/00958972.2015.1046852].

References

[1] K.H. Dötz. *Angew. Chem. Int. Ed.*, **23**, 587 (1984).
[2] S. Kotha, M.K. Dipak. *Tetrahedron*, **68**, 397 (2012).
[3] P. de Frémont, N. Marion, S.P. Nolan. *Coord. Chem. Rev.*, **253**, 862 (2009).
[4] K.H. Dötz, P. Tomuschat. *Chem. Soc. Rev.*, **28**, 187 (1999).
[5] D.M. Andrada, J.O.C. Jimenez-Halla, M. Solà. *J. Org. Chem.*, **75**, 5821 (2010).
[6] B. Heckl, H. Werner, E.O. Fischer. *Angew. Chem. Int. Ed. Engl.*, **7**, 817 (1968).
[7] B. Denise, P. Dubost, A. Parlier, M. Rudler, H. Rudler, J.C. Daran, J. Vaissermann, F. Delgado, A.R. Arevalo, R.A. Toscano, C. Alvarez. *J. Organomet. Chem.*, **418**, 377 (1991).
[8] E. Moser, E.O. Fischer. *J. Organomet. Chem.*, **16**, 275 (1969).
[9] E.W. Post, K.L. Watters. *Inorg. Chim. Acta*, **26**, 29 (1978).
[10] C.P. Casey, N.W. Vollendorf, K.J. Haller. *J. Am. Chem. Soc.*, **106**, 3754 (1984).
[11] E.O. Fischer, M. Leupold. *Chem. Ber.*, **105**, 599 (1972).
[12] E. Licandro, S. Maiorana, A. Papagni, P. Hellier, L. Capella, A. Persoons, S. Houbrechts. *J. Organomet. Chem.*, **583**, 111 (1999).
[13] B.A. Anderson, W.D. Wulff, T.S. Powers, S. Tribbitt, A.L. Rheingold. *J. Am. Chem. Soc.*, **114**, 10784 (1992).

[14] A. Parlier, H. Rudler, J.C. Daran, C. Alvarez. *J. Organomet. Chem.*, **333**, 245 (1987).
[15] M. Landman, R. Pretorius, B.E. Buitendach, P.H. van Rooyen, J. Conradie. *Organometallics*, **32**, 5491 (2013).
[16] H. Meerwein. *Org. Synth.*, **46**, 113 (1966).
[17] M. Landman, R Liu, R. Fraser, P.H. van Rooyen, J. Conradie. *J. Organomet. Chem.*, **752**, 171 (2014).
[18] R. Streubel, S. Priemer, F. Ruthe, P.G. Jones, D. Gudat. *Eur. J. Inorg. Chem.*, **5**, 575 (1998).
[19] S. Thompson, H.R. Wessels, R. Fraser, P.H. van Rooyen, D.C. Liles, M. Landman. *J. Mol. Struct.*, **1060**, 111 (2014).
[20] APEX2 (including SAINT and SADABS), Bruker AXS Inc., Madison, WI (2012).
[21] G.M. Sheldrick. *Acta Crystallogr. A*, **64**, 112 (2008).
[22] L.J. Farrugia. *J. Appl. Crystallogr.*, **30**, 565 (1997).
[23] C.J. Cason, POV-RAY for Windows, Persistence of Vision (2004).
[24] A.D. Becke. *Phys. Rev. A*, **38**, 3098 (1988).
[25] C.T. Lee, W.T. Yang, R.G. Parr. *Phys. Rev. B*, **37**, 785 (1988).
[26] M.J. Frisch, G.W. Trucks, H.B. Schlegel, G.E. Scuseria, M.A. Robb, J.R. Cheeseman, G. Scalmani, V. Barone, B. Mennucci, G.A. Petersson, H. Nakatsuji, M. Caricato, X. Li, H.P. Hratchian, A.F. Izmaylov, J. Bloino, G. Zheng, J.L. Sonnenberg, M. Hada, M. Ehara, K.Toyota, R. Fukuda, J. Hasegawa, M. Ishida, T. Nakajima, Y. Honda, O. Kitao, H. Nakai, T. Vreven, J.A. Montgomery Jr., J.E. Peralta, F. Ogliaro, M. Bearpark, J.J. Heyd, E. Brothers, K.N. Kudin, V.N. Staroverov, T. Keith, R. Kobayashi, J. Normand, K. Raghavachari, A. Rendell, J.C. Burant, S.S.Iyengar, J. Tomasi, M. Cossi, N.Rega, J.M. Millam, M. Klene, J.E. Knox, J.B.Cross, V. Bakken, C. Adamo, J.Jaramillo, R. Gomperts, R.E. Stratmann, O. Yazyev, A.J. Austin, R.Cammi, C. Pomelli, J.W. Ochterski, R.L. Martin, K. Morokuma, V.G. Zakrzewski, G.A. Voth, P. Salvador, J.J. Dannenberg, S. Dapprich, A.D. Daniels, O. Farkas, J.B. Foresman, J.V. Ortiz, J. Cioslowski, D.J. Fox, *Gaussian 09, Revision C.01*, Gaussian Inc., Wallingford, CT (2010).
[27] J.P. Perdew, J.A. Chevary, S.H. Vosko, K.A. Jackson, M.R. Pederson, D.J. Singh, C. Fiolhais. *Phys. Rev. B*, **46**, 6671 (1992). Erratum: J.P. Perdew, J.A. Chevary, S.H. Vosko, K.A. Jackson, M.R. Perderson, D.J. Singh, C. Fiolhais, Phys. Rev. B, **48**, 4978 (1993).
[28] G. te Velde, F.M. Bickelhaupt, E.J. Baerends, C. Fonseca Guerra, S.J.A. van Gisbergen, J.G. Snijders, T. Ziegler. *J. Comput. Chem.*, **22**, 931 (2001).
[29] C. Fonseca Guerra, J.G. Snijders, G. te Velde, E.J. Baerends. *Theor. Chem. Acc.*, **99**, 391 (1998).
[30] ADF2013.01, SCM, *Theoretical Chemistry*, Vrije Universiteit, Amsterdam, The Netherlands.
[31] F. Weigend, R. Ahlrichs. *Phys. Chem. Chem. Phys.*, **7**, 3297 (2005).
[32] J.A. Connor, E.M. Jones. *J. Chem. Soc. (A)*, **12**, 1974 (1971).
[33] S. Aoki, T. Fujimura, E. Nakamura. *J. Am. Chem. Soc.*, **114**, 2985 (1992).
[34] C. Crause, H. Görls, S. Lotz. *Dalton Trans.*, **9**, 1649 (2005).
[35] F. Fringuelli, S. Gronowitz, A.-B. Hörnfeldt, I. Johnson, A. Taticchi. *Acta Chem. Scand. B*, **28b**, 175 (1974).
[36] D.A. Forsyth, G.A. Olah. *J. Am. Chem. Soc.*, **101**, 5309 (1979).
[37] C.P. Butts, C.R. Jones, E.C. Towers, J.L. Flynn, L. Appleby, N.J. Barron. *Org. Biomol. Chem.*, **9**, 177 (2011).
[38] M. Landman, H. Görls, S. Lotz. *J. Organomet. Chem.*, **617–618**, 280 (2001).
[39] M. Landman, H. Görls, S. Lotz. *Eur. J. Inorg. Chem.*, 223 (2001).